Sonochemical Synthesis under a Magnetic Field: Structuring Magnetite Nanoparticles and the Destabilization of a Colloidal Magnetic Aqueous Solution under a Magnetic Field

ARTICLE *in* THE JOURNAL OF PHYSICAL CHEMISTRY C · DECEMBER 2007

Impact Factor: 4.77 · DOI: 10.1021/jp075637k

2 AUTHORS, INCLUDING:

A. Gedanken
Bar Ilan University
362 PUBLICATIONS **11,487** CITATIONS

SEE PROFILE

Sonochemical Synthesis under a Magnetic Field: Structuring Magnetite Nanoparticles and the Destabilization of a Colloidal Magnetic Aqueous Solution under a Magnetic Field

R. Abu-Much and A. Gedanken*

Department of Chemistry and Kanbar Laboratory for Nanomaterials at the Bar-Ilan University Center for Advanced Materials and Nanotechnology, Bar-Ilan University, Ramat-Gan, 52900, Israel

Received: July 18, 2007; In Final Form: October 18, 2007

This work is devoted to the investigation of the effect of an external magnetic field (MF) applied to a sonochemical synthesis. The paper presents results on the preparation of both aggregated magnetite nanoparticles and the destabilization of a magnetite hydrosol that is formed without a MF. The results reveal a difference in morphology, size, and magnetic properties of the product obtained under a MF. They also show that the applied magnetic field affects the stabilization mechanism of the magnetite particles in an aqueous solution and destroys the stable hydrosol formed without a MF. Instead, the formation of tree-like, aggregated structures composed of small particles is observed.

1. Introduction

The synthesis of uniformly sized magnetic nanoparticles has been intensively pursued because of their broad applications, including magnetic storage media, ferrofluids, magnetic resonance imaging, and magnetically guided drug delivery.[1] Various methods have been reported for the synthesis of metal oxide nanoparticles, such as flame pyrolysis,[2] sol−gel reactions,[3,4] and chemical oxidation in micellar media or in polymer or mineral matrixes.[5]

The most common techniques for the synthesis of magnetite nanoparticles in aqueous solutions are based on the wet-chemical coprecipitation of ferrous and ferric ions. The coprecipitation is conducted with the addition of ammonia or sodium hydroxide to the aqueous solution or to the microemulsion.[6,7] The partial oxidation of ferrous hydroxide gels,[8,9] spray pyrolysis, and ion exchange, are other methods for magnetite preparation.[10−12] The synthesis of the stable hydrosol by a one-step process is one of the main challenges, and a number of methods were reported on this topic in the literature.[13−25] However, in all these cases, coating was accomplished ex situ, that is, the nanoparticles were prepared first and then subjected to the surfactant solution under agitation.

Little attention has been paid to the effect of an external magnetic field on the nucleation and growth process of magnetic particles and on the self-assembly behavior of magnetic nanocrystallites. It has been indeed found that the magnetic field can significantly influence the movement of magnetic particles.[27−29] It is, therefore, very interesting to study the growth behavior of magnetic particles during their fabrication under an external magnetic field. Recent developments have indicated that the magnetic field, as an elegant way, could be applied to orient and self-assemble magnetic nanoparticles into nano- or microscale structures in which dipole interactions between adjacent magnetic nanoparticles couple them together and force the reversible formation of an anisotropic structure.[30−33] These magnetic nanoparticles, as a system of wide research interest, encompass fascinating aspects including superparamagnetism, dipolar interactions, and Zeeman energy. Three-dimensional (3D), as well as two- and one-dimensional self-assembled structures of magnetic nanoparticles, have been synthesized through magnetic interactions and the application of a magnetic field.[34−40]

Power ultrasound influences chemical reactivity through an effect known as "cavitation". Cavitation occurs by applying high-intensity ultrasound to liquids, resulting in the superposition of sinusoidal pressure on the steady ambient pressure. Sound is transmitted through a fluid as a wave consisting of alternating compression and refraction cycles. In the cavitation phenomenon, the microbubbles formed during the refraction cycle of the acoustic wave undergo a violent collapse during the compression cycle of the wave. The bubble's content is estimated to be heated to 5000 K, and the implosion of the cavitation bubble also produces high-energy shock waves with pressures of several thousand atmospheres.[41] The ultimate consequence of the high temperature is a chemical reaction. The high pressure leads also to an increased number of molecular collisions owing to enhanced molecular mobility and decreased overall volume, leading also to high chemical reactivity.

Recently, we have reported on a sonochemical method for the synthesis of both aggregated magnetite nanoparticles and their stable aqueous dispersion by a direct one-step process.[26] Poly(vinyl alcohol) (PVA) is used both as a stabilizer and as a protecting layer against oxidation by the use of high-intensity ultrasound. The current work is centered on the investigation of the effect of applying an external magnetic field during this synthesis; the same reactions were carried out while the sonication cell was placed between the poles of a magnetic field.

2. Experimental Section

2.1. Chemicals. The precursors for this study were iron(II) acetate, 99.995% (Aldrich), and poly(vinyl alcohol) (Fluka). These chemicals were used without further purification.

2.2. Experimental Procedure. The experiment can be divided into two sections. In the first, we investigated the application of a magnetic field during the sonochemical synthesis of aggregated magnetite particles; in the second, we studied the effect of a magnetic field on the stabilization mechanism of these particles. The process of regular sonochem-

* To whom correspondence should be addressed.

10.1021/jp075637k CCC: $40.75
Published on Web 12/11/2007

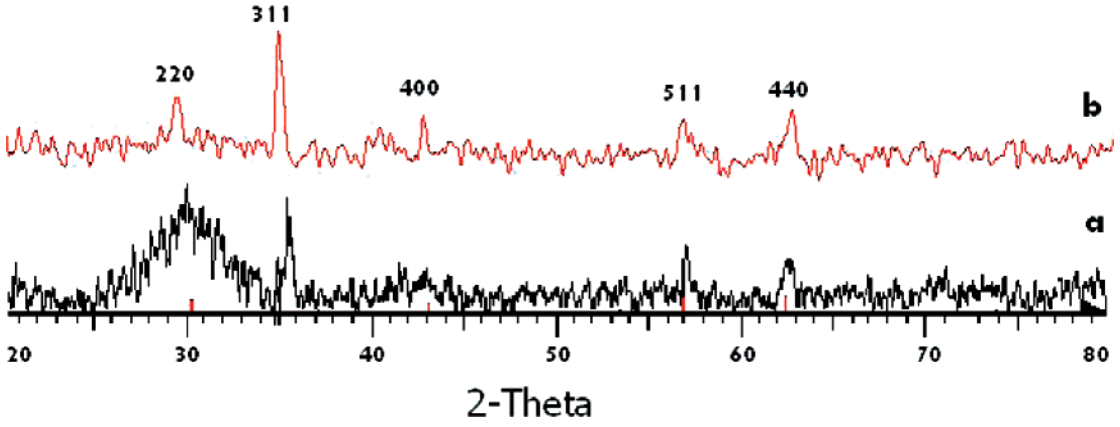

Figure 1. (a) XRD pattern of magnetite particles obtained by a regular sonication process, and (b) XRD pattern of magnetite particles synthesized under an external magnetic field.

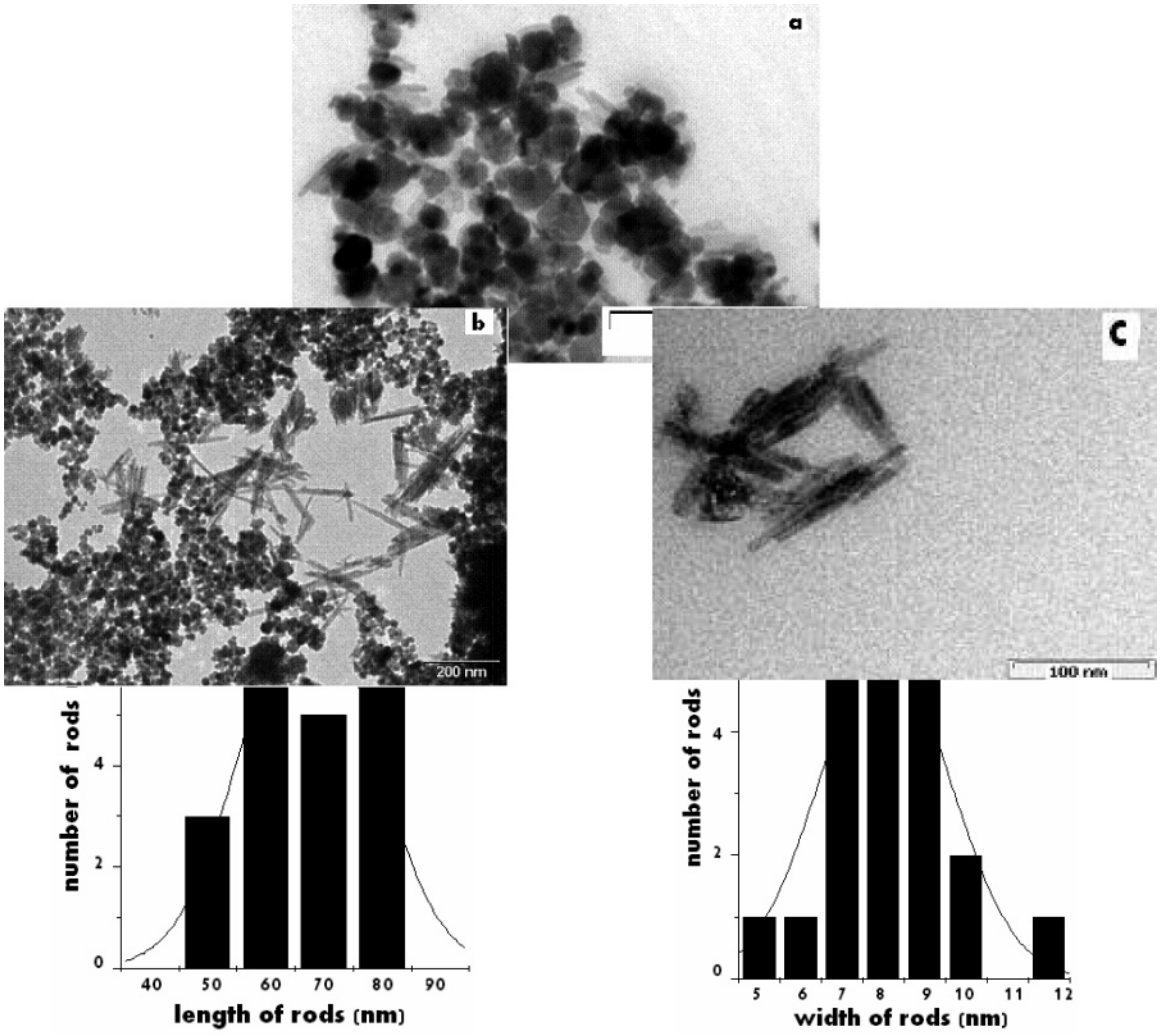

Figure 2. TEM images of magnetite particles: (a) magnetite particles synthesized using the regular sonication procedure, (b) magnetite prepared in the presence of a 0.1 T magnetic field, (c) magnetite prepared in the presence of a 0.5 T magnetic field, (d) average length of rods obtained under a 0.5 T magnetic field, and (e) average width of rods obtained under a 0.5 T magnetic field.

ical synthesis and the chemical reaction mechanism have been described by us elsewhere.[26,56] Briefly, a double-distilled deoxygenated water solution of 0.1 M iron(II) acetate was subjected to a high-intensity ultrasonic horn (Ti-horn, 20 kHz) under 1.2 atm of Ar for 15 min. By the same procedure, a stable aqueous solution was obtained by the addition of 0.000066 M, PVA (100 000), prior to the sonication. Similarly, the same sonochemical reactions were performed in the presence of an applied external magnetic field of 0.5 T. In both cases, the powder obtained was centrifuged, washed repeatedly with double-distilled deoxygenated water, and finally washed with dry pentane in an inert glovebox (O_2 < 1 ppm) and dried under vacuum.

2.3. Analysis and Characterization. The powder X-ray diffraction measurements were carried out using a model-2028 (Rigaku) diffractometer (using Cu Kα = 1.5418 Å radiation).

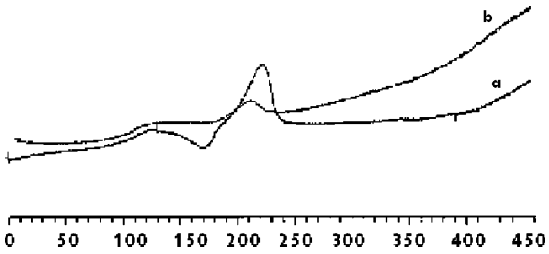

Figure 3. DSC spectra of (a) magnetite particles prepared using the regular sonication procedure, and (b) magnetite particles prepared in the presence of an applied magnetic field.

The morphology and the structure of the as-synthesized products were further characterized with a JEM-1200EX TEM and a JEOL-2010 HRTEM. Samples for TEM and HRTEM were prepared by dispersing the products into ethanol, placing a drop of this suspension onto a copper grid coated with an amorphous carbon film, and then drying under an inert atmosphere. The thermal analysis of differential scanning calorimetry (DSC) was conducted by a Mettler Toledo DSC 25. The samples were heated to 550 °C at a rate of 10 °C/min under a nitrogen atmosphere. Magnetization was measured using a Quantum Design MPMS SQUID (superconducting quantum interference device) magnetometer. First, the blocking temperature was measured by cooling the sample in zero field down to 5 K, at which point a magnetic field of 100 Oe was applied. After that, the sample was slowly warmed to a high temperature in steps of a few Kelvin, with stabilization at each temperature range, and subsequent measurements of the magnetic moment (this is the so-called zero-field cooled measurement (ZFC)). Then, without turning off the magnetic field, the sample was cooled with measurements of the magnetic moment at each intermediate temperature (field-cooled measurements (FC)).

3. Results and Discussion

3.1. Investigation of the Effect of Applying an External Magnetic Field during the Sonochemical Synthesis of Fe_3O_4 Nanoparticle Powder. The XRD patterns of the products prepared with and without an external magnetic field applied are presented in parts b and a of Figure 1, respectively. Both samples show diffraction peaks assigned to face-centered-cubic magnetite. The sample prepared under a MF shows some sharper crystalline peaks, which might originate from the oriented growth of the particles induced by the applied magnetic field.

Figure 2, parts a−c, depicts the TEM images of samples obtained using sonication in the absence of a magnetic field (Figure 2a) and with applied magnetic fields (Figure 2, parts b and c) of 0.1 and 0.5 T, respectively. There is an obvious difference not only in the particle shape but also in particle size. The morphology of the particles obtained without a magnetic field is that of spherically shaped particles with an average diameter of ∼23 nm, calculated by using Scion Image Software. In addition to spherical particles, rod-like structures were obtained when a 0.1 T magnetic field was applied (Figure 2b). When the strength of the magnetic field was increased to 0.5 T, only rod-like structures were formed, accompanied by the disappearance of the spherical particles (Figure 2c). The dimensions of the rods were the following: average length = 69 nm (Figure 2d), and average diameter = 7.9 nm (Figure 2e, calculated by using Scion Image software).

Basically, the growth process of the particles has a crucial role in determining the shape and size of the particles. The application of an external magnetic field affects the growth process of the particles. In most of the cases, the particle growth is a diffusion-assisted process. In such cases, the magnetic field determines the preferable direction for the motion of the magnetic atoms, hence assisting the growth in that direction. In addition, the direct magnetic interactions between the particles are more significant, and they also have a crucial role in the morphology and the size of the particles.

The DSC trace of the products obtained without and with a magnetic field is depicted in Figure 3, parts a and b, respectively; both samples exhibited an exothermic peak at 215 °C. The exothermic peak did not appear in a second heating cycle, indicating that part of the magnetite was formed as an amorphous product. It is worth noting that the magnitude of the heat evolved when the sample was prepared under a magnetic field is smaller than that released when the reaction

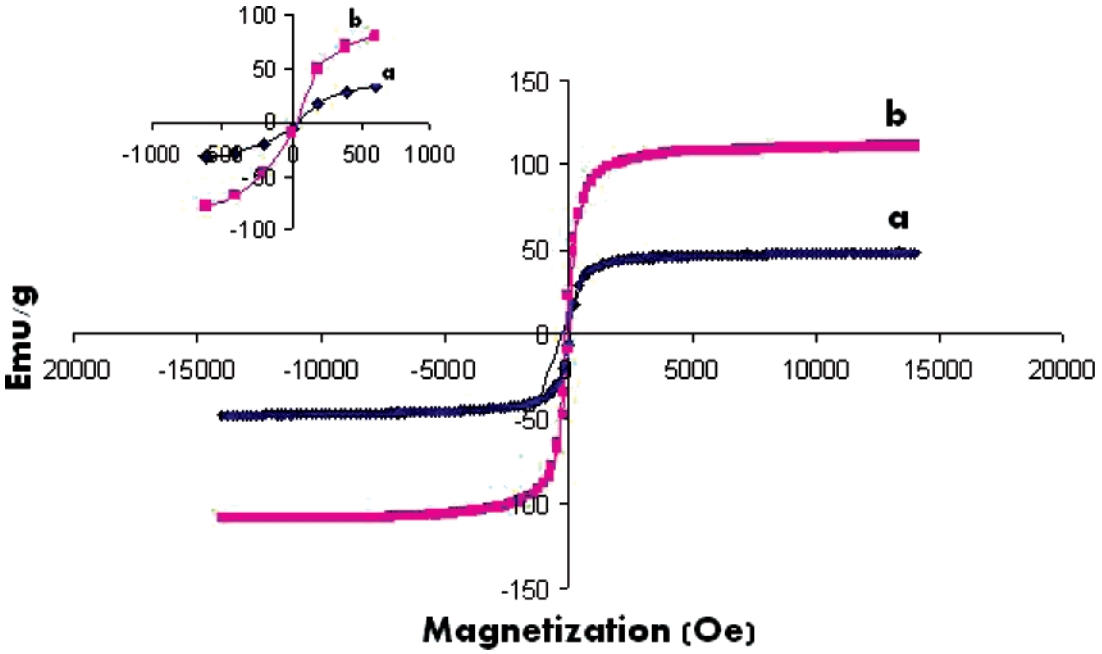

Figure 4. (a) Magnetization loop of magnetite particles obtained without a magnetic field, and (b) magnetization loop of magnetite particles obtained under an external magnetic field.

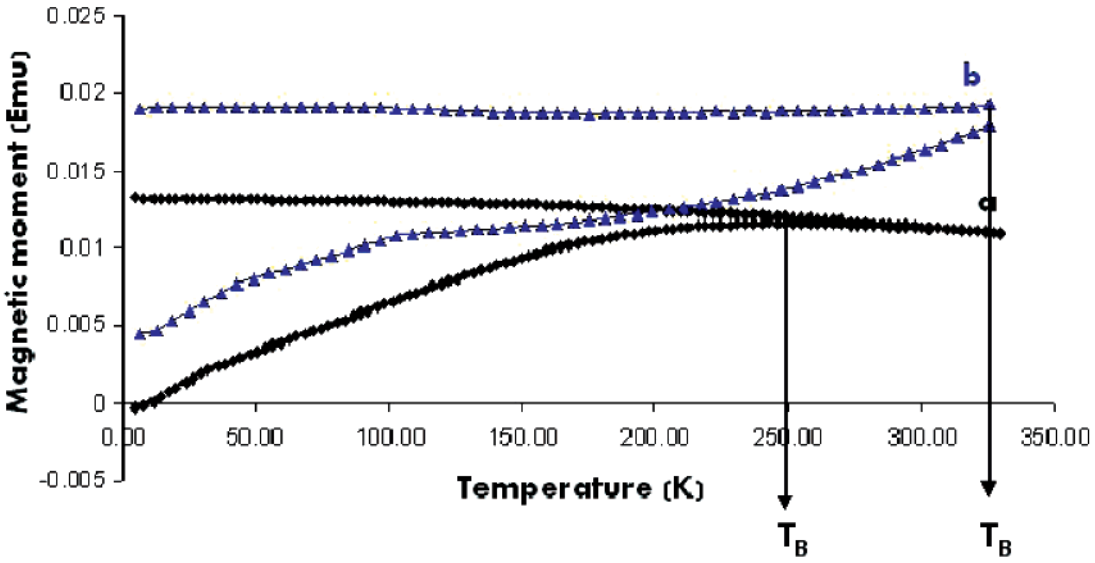

Figure 5. Magnetic moment versus temperature measurements for (a) magnetite particles prepared without an applied magnetic field, and (b) magnetite particles prepared under a magnetic field.

is conducted without a MF. This is interpreted as representing a larger size of the crystalline domains obtained when a MF is employed. The effect of a magnetic field on crystallization is known, and similar results are reported in refs 52 and 53.

The difference in the morphology and size of the magnetite particles obtained by conducting the same sonochemical reaction under an external magnetic field is reflected in the differences in the magnetic properties.

Figure 4, parts a and b, depicts the magnetization loops of Fe_3O_4 both synthesized by a regular sonication and under the application of an external magnetic field, respectively. They exhibit the obvious difference in the saturation magnetization (M_s) between the sample derived under an external magnetic field (~80 emu/g) and the sample obtained without an applied magnetic field (~50 emu/g). As evidenced from the expanded insert of Figure 4, no hysteresis is found for the two samples. The difference in the M_s between the samples prepared with and without a MF can be attributed to spin disorder and surface oxidation. The magnetic behavior of nanoparticles has a marked dependence on the decrease in particle size and when the surface effects start to dominate.[42] In nanoparticles with a large surface/volume ratio, the surface-spin-driven arrangements (spin disorder) may eventually modify the magnetic properties. This spin disorder is caused by a lower coordination of the surface atoms, broken exchange bonds that produce a spin glass-like state of spatially disordered spins on the surface with a high-anisotropy surface layer.[43−44] In addition, the change in the magnetic structure can also be the reason, when a magnetic field is applied, that the magnetic easy axes of magnetite could be aligned along the rod-like structures. This can also be responsible for the increase in the saturation magnetization. Finally, perhaps this difference arises from the crystallization effect discussed above. It is well-known that the saturation magnetization (Ms) of amorphous iron is much smaller than that of crystalline iron. Since we argued that the magnetic field caused almost the elimination of the amorphous product, higher Ms values are obtained for almost a fully crystalline product.

We have also conducted measurements of the magnetic moment as a function of temperature. First, the magnetization was measured by two different procedures. (1) The sample was zero-field-cooled (ZFC) to 5 K; a field was applied, and the magnetization was measured as a function of temperature. (2) The sample was field-cooled (FC) from above 300 to 5 K and the magnetization was measured. (3) The sample was field-cooled to 5 K, after which the field was reversed in sign and the magnetization was measured as a function of temperature (RFC). The results are shown in Figure 5, parts a and b. By increasing the temperature of the sample, more thermal energy is available to disturb the system. Therefore, more magnetic moments will align along the external magnetic field direction. Eventually, the net moment of the system will reach a maximum where the greatest population of moments has aligned along the external field. The peak temperature is called the blocking temperature (T_B). As the temperature rises above T_B, thermal vibrations become strong enough to randomize the moments. Below the blocking temperature, T_B, ZFC and FC curves do not coincide. Above T_B, they coincide, and the materials exhibit a superparamagnetic behavior. According to Figure 5a, the blocking temperature of the sample obtained without a magnetic field ($\sim T_B = 250$ K) is lower than that of the sample synthesized in the presence of a magnetic field ($\sim T_B > 325$ K). This difference is accounted for by the relation of T_B, which is known to depend on $T_B = KV/25k$, where K is the effective uniaxial anisotropy energy per unit volume, V is the particle's volume, and k is the Boltzmann constant. It is clear that the K of the rods obtained when the MF is applied is larger than that of the K of the reaction without a magnetic field. The blocking temperature is therefore higher for these rods. The blocking temperature also depends on size, shape, and the material. It usually increases as the particle size increases.[55] Nanorods usually have a higher blocking temperature than nanodots.

3.2. Investigation of the Effect of Applying an External Magnetic Field on the Stabilization Mechanism of Fe_3O_4 by Interaction with PVA. It was reported recently by us[26] that the addition of a desired amount of PVA-100 000 during the sonochemical synthesis of the magnetite nanoparticles leads to the fabrication of a stable hydrosol, so that as soon as the Fe_3O_4 particles are formed they are almost simultaneously coated with PVA, which acts as a protective shell against aggregation. In the process presented here, we have destroyed the stabilization layer around the magnetite nanoparticles by applying an external magnetic field during the sonochemical reaction, and no stable dispersion of magnetite nanoparticles is observed. After the end of sonication, we could detect a black precipitate at the bottom

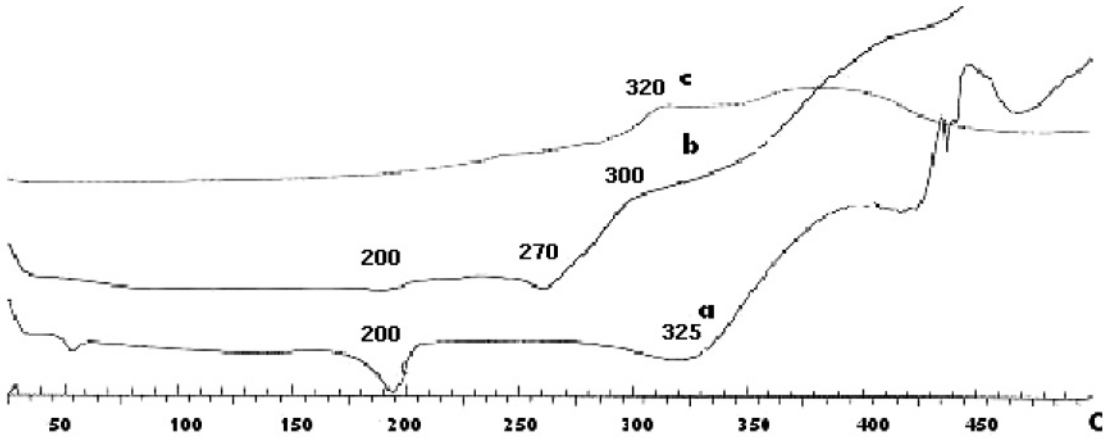

Figure 6. (a) DSC trace of pristine PVA, (b) DSC trace of magnetite−PVA nanocomposites prepared by a regular sonication procedure, and (c) DSC trace of magnetite particles prepared by sonication under a magnetic field with addition of PVA.

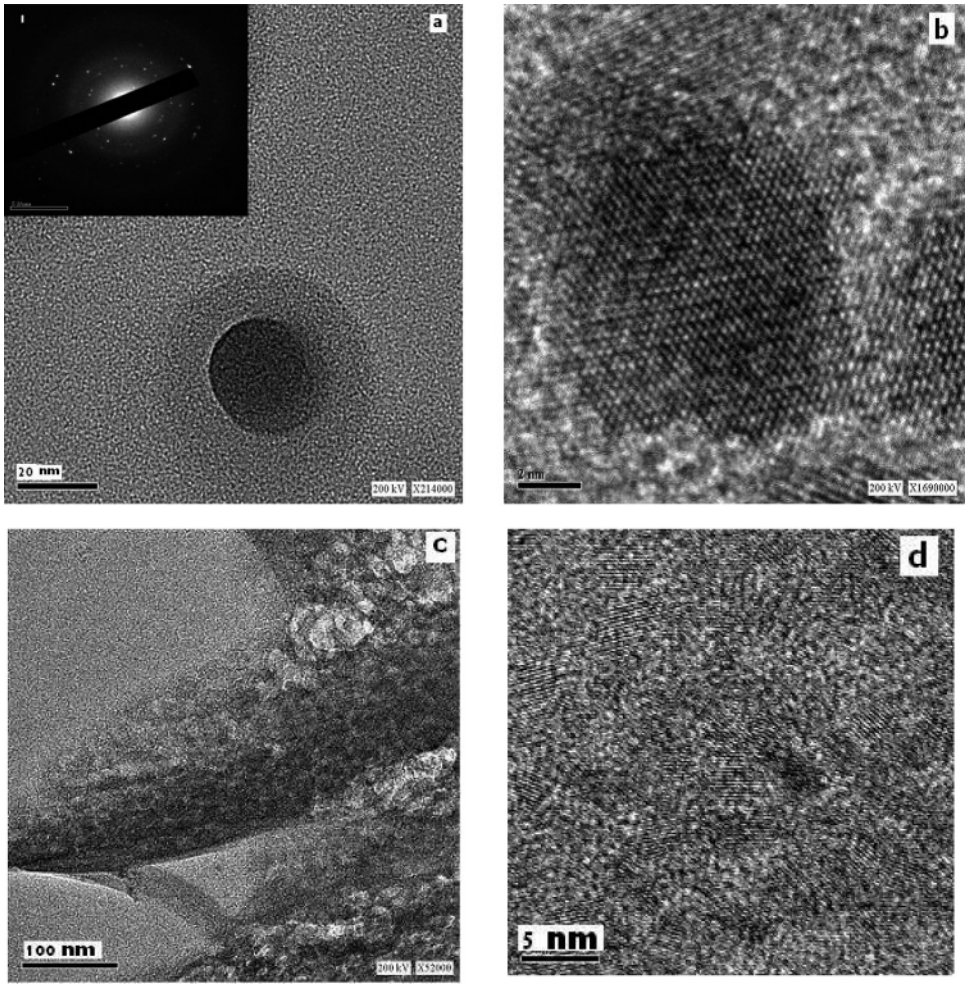

Figure 7. HRa TEM micrographs of (a,b) single particle obtained without a magnetic field, (c) aggregated particles obtained under a magnetic field, and (d) high magnification of image 7(c).

of the reaction vessel. Identical morphological results and thermal properties were obtained upon using different concentrations of PVA. These conclusions are based on DSC, EDAX, and indirectly by HRTEM measurements.

Figure 6, parts a−c, depicts the DSC plots for pristine PVA, the nanocomposites obtained in the absence of a magnetic field, and the aggregated nanoparticles obtained by sonication under an external magnetic field of 0.5 T, respectively. In plots a and b, we could detect peaks corresponding to the thermal transitions of PVA. Both curves show endothermic peaks at ∼200 °C that are attributed to the loss of bonded water. The second endothermic peaks are assigned to the structural decomposition of the polyvinyl alcohol. It can also be seen that the interaction between the magnetite particles and PVA has weakened the interchain interactions and leads to polymer decomposition at lower temperatures. However, in the aggregated product obtained by applying a MF, there is no detection of thermal peaks assigned to PVA (Figure 6c). It is suggested that the interaction of the fabricated magnetite particles with the magnetic field during the sonication procedure acts as a barrier against the adsorption or chemical attachment of the PVA molecules, resulting in an aggregation process.

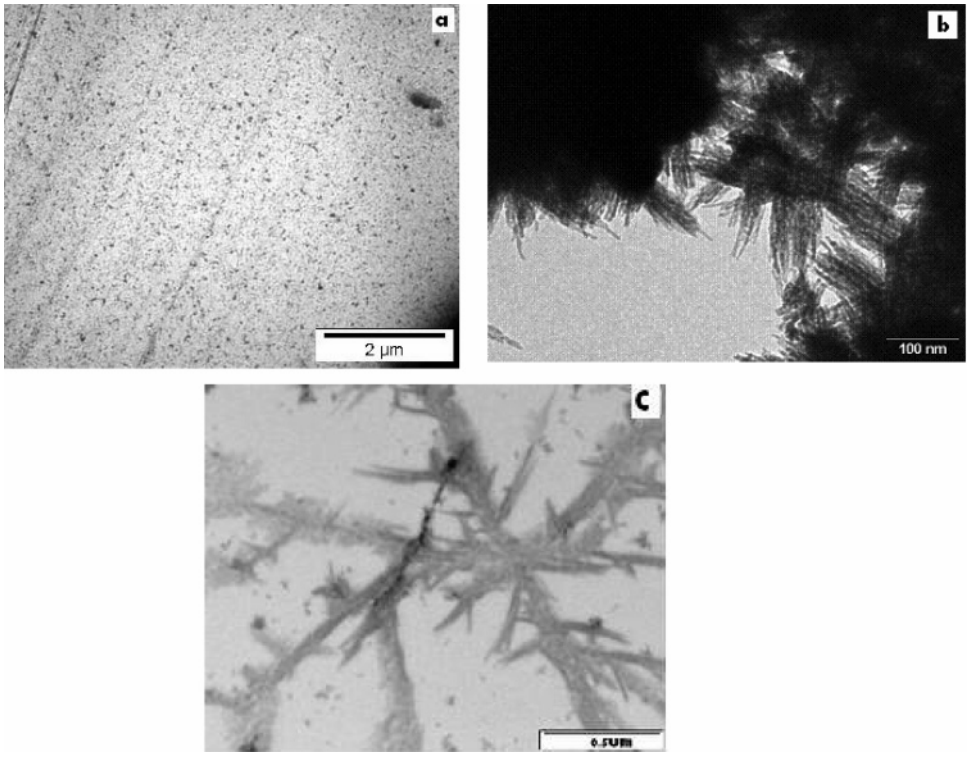

Figure 8. Transmission electron micrographs of (a) well-dispersed Fe_3O_4 obtained by sonication in the absence of a magnetic field, (b) aggregated Fe_3O_4 obtained after sonication under a 0.1 T external magnetic field, and (c) tree-like aggregates obtained by sonication under a 0.5 T magnetic field.

Further support for the disappearance of the PVA shell surrounding the aggregated particles obtained under a MF is realized by a comparison between the HRTEM images of stable particles produced by a regular sonication process (Figure 7a) and the aggregated particles obtained under a MF. In Figure 7a, we could detect a shell surrounding the particles; it is assigned to the chains of the PVA polymer that are adsorbed to the surface of the magnetite particles and prevent them from agglomeration. By contrast, we could not observe any surrounding shell around the particles obtained under a MF. Preventing the formation of the shell resulted in particle aggregation (Figure 7, parts c and d). The figure also illustrates the perfect arrangement of the atomic layers of magnetite. The SAEDS results related to the aggregated particles revealed a significant decrease in the amount of carbon, in comparison with the stable particles.[26] In addition, the C and H analysis shows that the content of the carbon is lower than 5 as compared to 30 wt %.[26] This dramatic reduction in the carbon content indicates clearly that the precipitation is not a result of aggregation caused by the magnetic field, but is due to the avoidance of the surfactant coating caused by the magnetic field.

The morphology of the aggregated particles compared to the separated ones obtained without a MF was also studied. Figure 8a shows well-dispersed particles obtained in the absence of a magnetic field, whereas a different aggregation mode is formed when 0.1 and 0.5 T magnetic fields are applied (Figure 8, parts b and c, respectively). Applying a more intense magnetic field (0.5 T) resulted in the precipitation of tree-like structures.

The magnetization of ferromagnetic magnetite bulk material is very sensitive to the microstructure of the sample. Superparamagnetism occurs when the particle is small enough so that thermal fluctuations (of the order of kT) can overcome the magnetic anisotropy (which is proportional to the particle's volume). Once this happens, the magnetization of the particle is no longer fixed along a certain direction (determined by the easy magnetic direction of the lattice), but processes at random, as each particle acts as a big "spin" with a suppressed exchange interaction between the particles. The lack of hysteresis is one of the criteria required for the identification of the product as superparamagnetic. We performed room-temperature magnetization (Figure 9) measurements of the Fe_3O_4−PVA nanocomposites which were prepared by regular sonication (average size ∼23 nm), as well as of aggregated small particles which were produced under an external magnetic field with the addition of PVA. The results are presented in Figure 9, parts a and b, respectively. It is seen that the Fe_3O_4−PVA nanocomposites (Figure 9a) do not show hysteresis, and their saturation magnetization (Ms) is lower than that obtained under a magnetic field. This can be attributed to the existence of a nonmagnetic "dead layer" of PVA, causing a quenching of the magnetization. The remaining question is why the Ms is smaller than the values measured for pristine magnetite. We associate this low value of Ms to the small size of the particles.

3.3. Discussion. The extreme conditions occurring when the bubble collapses might lead to the assumption that what determines the shape and size of the reaction product is sonochemistry, and the application of a magnetic field during sonication would have only a minor effect. This is especially true since the magnetic dipole formula does not contain the external magnetic field and is proportional only to $\mu_1 \cdot \mu_2/R^3$ $\{2 \cos(\theta_1 - \theta_2) - 3 \cos \theta_1 \cos \theta_2\}$.[54] However, the current result reveals the important role of the MF in determining the shape and magnetic properties of the products. Our explanation of these results is based on the place where the sonochemistry reaction occurs. This ionic reaction, whose mechanism was discussed previously,[41] takes place in the interfacial region of about 200 nm surrounding the collapsing bubble[41] at temperatures and pressures much lower than those developed at the center of the bubble. This diminishes the effect of the ultrasonic event in comparison with a gas-phase reaction that happens with

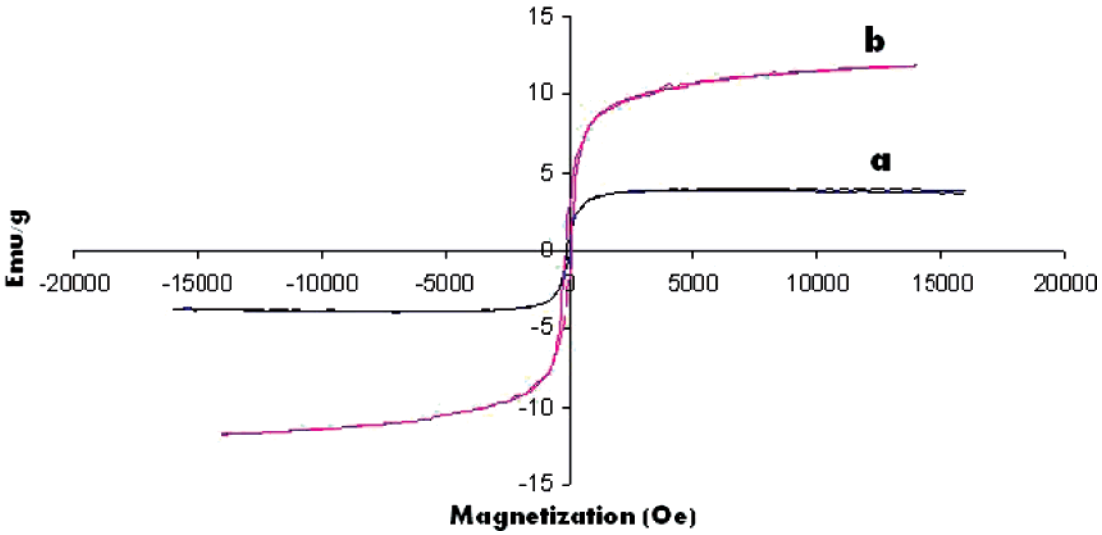

Figure 9. (a) Magnetization loop of magnetite−PVA nanocomposites, and (b) magnetization loop of magnetite particles prepared under a 0.5 T magnetic field.

a volatile precursor. The *R* in the denominator might also contribute to the importance of the magnetic field.

By the application of an external magnetic field during the growth of ferromagnetic particles, the particle growth is considered to be a diffusion-assisted slow process. Our investigation revealed that the extreme conditions resulting from the sonication cannot act as a barrier against the effect of a magnetic field on the growth process of the magnetite particles. The magnetic field led to the formation of rod-like, rather than spherically shaped, particles.

The more dramatic effect of the external magnetic field is seen in the interaction of the magnetite particles with PVA, when no colloidal solution is obtained, and the external magnetic field causes the destabilization of the colloidal solution. Owing to the low vapor pressure of the polymer, it exists either in the interfacial region or in the bulk. In other words, it is found in the region where the nucleation and growth process take place. Our explanation for the destruction of the stabilization layer is based on kinetic and thermodynamics arguments. We argue that the augmentation of the magnetite particles is faster than the capping process. In addition, the application of an external magnetic field causes the particles to attain large magnetic moments aligned in the direction of the magnetic field, resulting in a strong magnetic interaction, stronger than the interaction with PVA. The intensity of the interparticle magnetic attraction dominates over other colloidal interactions.

The results reveal that unique tree-like structures are formed under the application of a 0.5 T magnetic field. These structures were stable for several months even after centrifugation. Different theoretical approaches were offered toward the elucidation of these structures. Theoretical treatments are in agreement that the principle growth characteristics are the approximate constant velocity and paraboloidal shape of the tip, and the evenly spaced side branches that began to produce their own secondary side branches as they grow.[49] Pieters and Langer[50] were the first to suggest that side branches might be understood as a response of the system to noise. Numerical methods have been used to investigate the effects of noise, and they have revealed that the steady-state response of the system to noise is a plane wave. Thus, if we drive the system to a source of noise, the system at large distances will be a plane wave of a unique wave vector. We believe that once the noise amplitude increases beyond a small value, nonlinear effects will stabilize the perturbation and side branches will be observed. Diffusion-limited aggregation (DLA), introduced by Witten and Sander,[51] exhibits a satisfying model to study aggregation processes. It represents noisy growth limited by diffusion that consists of a single cluster, which grows by the attachment of random walkers to its boundary. According to our explanation, once the particles are formed, their motion is affected by the strong attraction to the magnetic field direction. However, it is restricted by their collision with the PVA chains. We assume the existence of a situation of competition between the interaction with the magnetic field and the adsorption or chemical attachment to the polymer in order to obtain a stable solution, but the magnetic interactions dominate. However, we cannot ignore the influence of the long chains of PVA in the solution on the specific mode of diffusion, which exist as a perturbation. The finite structure of the aggregated particles is also a function of a combination between the collisions with the PVA chains and the attraction toward the magnetic field. The entire situation supplies the desired parameters for the unique mode of aggregation and fabrication of tree-like structures. The restricted motion of the particles was also supported by their small size.

References and Notes

(1) (a) Sun, S.; Murray, C. B.; Weller, D.; Folks, L.; Moser, L. *Science* **2000**, *287*, 1989. (b) Awschalom, D.; Divicenzo, D. P. *Phys. Today* **1995**, *4*, 43. (c) Leslie-Pelecky, D.; Rieke, R. D. *Chem. Mater.* **1996**, *8*, 1770. (d) Raj, K.; Moskowitz, R. *J. Magn. Magn. Mater.* **1990**, *85*, 233. (e) Speliotis, D. E. *J. Magn. Magn. Mater.* **1999**, *193*, 29. (f) Raj, K.; Mostowitz, B.; Casciari, R. *J. Magn. Magn. Mater.* **1995**, *149*, 174. (g) Oswald, P.; Clement, O.; Chambon, C.; Schuman-Claeys, E. *Magn. Reson. Imaging* **1997**, 151025. (h) Berry, C.; Curtis, A. *J. Phys. D: Appl. Phys.* **2003**, *36*, R182.

(2) Grimm, S.; Schultz, M.; Barth, S.; Muller, R. *J. Mater. Sci.* **1997**, *32*, 1083.

(3) Stober, W.; Fink, A.; Bohn, E. *J. Colloid Interface Sci.* **1986**, *26*, 62.

(4) Jean, J.; Ring, H. *Langmuir* **1986**, *2*, 251.

(5) Mounien, N.; Pileni, M. P. *Chem. Mater.* **1996**, *8*, 1128.

(6) Jolivet, J. P.; Tronc, E.; Barbe, C.; Livage, J. *J. Colloid Interface Sci.* **1990**, *138*, 465.

(7) Massart, R. *IEEE Trans. Magn.* **1981**, *17*, 1247.

(8) Sidju, P. S.; Gilkes, R. J.; Posner, A. M. *J. Inorg. Nucl. Chem.* **1977**, *39* (11), 1953.

(9) Yang, D.; Ren, S.; Kann, G.; Zhou, D.; Li, M. *J. Colloid Interface Sci.* **1999**, *215*, 190.

(10) Yitai, Q.; Yi, X.; Chuan, H.; Jing, L.; Zuyao, C. *Mater. Res. Bull.* **1994**, *29* (9), 953.

(11) Gonzalez-Carreno, T.; Mifsud, A.; Serna, C. J.; Palacios, J. M. *Mater. Chem. Phys.* **1991**, *27*, 287.

(12) Ziolo, R. F.; Giannelis, E. B.; Weinstein, B. A.; O'Horo, M. P.; Ganguly, B. N.; Mehrotra, V.; Russell, M. W.; Huffman, D. R. *Science* **1992**, *257*, 219.
(13) Bonnemann, H.; Richards, R. M. *Eur. J. Inorg. Chem.* **2001**, 2455.
(14) Sahoo, Y. J. *Phys. Chem. B* **2005**.
(15) Bacri, J.; Perzynski, R.; Salin, D.; Cabuil, V.; Massart, R. *J. Magn. Mater.***1990**, *318*, 85, 27.
(16) Khalafalla, S.; Reimers, G. W. *IEEE Trans. Magn. Mag.* **1980**, *16*, 178.
(17) Shen, L.; Stachowiak, A.; Seif-Edden, K. F.; Laibinis, P.; Hatton, E. *Langmuir*, **2001**, *17*, 288.
(18) Shimoizaka, J.; Nakatsuka, K.; Fujita, T.; Kounosu, A. *IEEE Trans. Magn. Mag.* **1980**, *16*, 368.
(19) Wormuth, K. *J. Colloid Interface Sci.* **2001**, *241*, 366.
(20) Pardoe, H.; Chau-Anusorn, W.; Pierre, T. G.; Dobson, J. *J. Magn. Magn. Mater.* **2001**, *255*, 41.
(21) Mendenhall, G. D.; Geng, Y.; Hwang, J. *J. Colloid Interface Sci.* **1996**, *184*, 519.
(22) Lee, J.; Isobe, T.; Senna, M. *J. Colloid Interface Sci.* **1996**, *177*, 490.
(23) Palmacci, S.; Josephon, L.; Groman, E. V. *Synthesis of Polymer Covered Superparamagnetic Oxide Colloids for Magnetic Resonance Contrast Agents or Other Applications, PCT WO 9505669* **1993**, *8*, 12.
(24) Ding, X. B.; Sun, Z. H.; Wan, G. X.; Jiang, Y. Y. *React. Funct. Polym.* **1998**, *38*, 11.
(25) Underhill, R. S.; Liu, G. *Chem. Mater.* **2000**, *12*, 2082.
(26) Abu-Much, R.; Meridor, U.; Frydman, A.; Gedanken, A. *J. Phys. Chem. B* **2006**, *110*, 8194.
(27) Chudnovsky, E. M. *J. Magn. Magn. Mater.* **1998**, *185*, L267.
(28) Zhang, X.; Wei, H. L.; Zhang, Z. Q.; Zhang, L. *Phys. Rev. Lett.* **2001**, 87, 157203.
(29) Wu, X. W.; Liu, C.; Li, L.; Jones, P.; Chantrell, R. W.; Weller, D. *J. Appl. Phys.* **2004**, *95*, 6810.
(30) Furst, E. M.; Suzuki, C.; Fermigier, M.; Gast, A. p. *Langmuir* **1998**, *14*, 7334.
(31) Niu, H.; Chen, Q.; Ning, M.; Jia, Y.; Wang, X. *J. Phys. Chem. B* **2004**, *108*, 3996.
(32) Sheparovych, R.; Sahoo, Y.; Motornov, M.; Wang, S.; Luo, H.; Prasad, P. N.; Sokolov, I.; Minko, S. *Chem. Mater.* **2006**, *18*, 591.
(33) Vuppu, A. K.; Garcia, A. A.; Hayes, M. A. *Langmuir* **2003**, *19*, 8646.
(34) Sun, S. *Adv. Mater.* **2006**, *18*, 393.
(35) Love, J. C.; Urbach, A. R.; Prentiss, M. G.; Whitesides, G. M. *J. Am. Chem. Soc.* **2003**, *125*, 12696.
(36) Grzybowski, B. A.; Stone, H.; Whitesides, G. *Nature* **2000**, *405*, 1033.
(37) Tang, Z. Y.; Kotov, N. *Adv. Mater.* **2005**, *17*, 951.
(38) Boal, A. K.; Frankamp, B. L.; Uzun, O.; Tuominen, M. T.; Rotello, V. M. *Chem. Mater.* **2004**, *16*, 3252.
(39) Fried, T.; Shemer, G.; Markovich, G. *Adv. Mater.* **2001**, *13*, 1158.
(40) Gao, J.; Zhang, B.; Zhang, X.; Xu, B. *Angew. Chem., Int. Ed.* **2006**, *45*, 1220.
(41) Srivastava, D. N.; Perkas, N.; Zaban, A.; Gedanken, A. *Pure Appl. Chem.* **2002**, *74*, 1509.
(42) McHenry, M. E.; Loughin, D. E. *Acta Mater.* **2000**, *48*, 223.
(43) Kodama, R. H. *J. Magn. Magn. Mater.* **1999**, *200*, 359.
(44) Berkowitz, A. E.; Kodama, R. H.; Makhlouf, S. A.; Parker, F. T.; Spada, F. E.; McNiff, E. J.; Foner, S. *J. Magn. Magn. Mater.* **1999**, *196*, 591.
(45) Gambardella, F., et al. *Science* **2003**, *300*, 1130.
(46) Viota, J. L.; Vicente, J.; Duran, J. D. G.; Delgado, A. V. *J. Colloid Interface Sci.* **2005**, *284*, 527.
(47) Mendelev, V.; Ivanov, A. *J. Magn. Magn. Mater.* **2005**, *289*, 211.
(48) Rotariu, O.; Strachan, N. J. C. *Powder Technol.* **2003**, *132*, 226.
(49) Kessler, D.; Koplik, J.; Levine, H. *Adv. Phys.* **1988**, *37*, 255.
(50) Pieters, R.; Langer, J. S. *Phys. Rev. Lett.* **1986**, *56*, 1948.
(51) Witten, T. A.; Sander, L. M. *Phys. Rev. B* **1983**, *27*, 5696.
(52) Wang, Z. Y.; Xu, H.; Ni, J.; Li, Q.; Zhou, B. X. *Rare Met.* **2006**, *24* (4), 337.
(53) Fujij, H.; Tsurekawas, S.; Matsuzaki, T. *Philos. Mag. Lett.* **2006**, *86* (2), 113.
(54) Cullity, B. D. *Introd. Magn. Mater.* **1972**, 616.
(55) Chen, J. B.; Sorensen, C. M.; Klabunde, K. J.; Hadjipanayis, G. C. *Phys. Rev. B* **1995**, *51*, 11527.
(56) Vijayakumer, R.; Koltype, Yu.; Felner, I.; Gedanken, A. *Mater. Sci. Eng.* **2000**, *A286*, 101.